



Discover Generics

Cost-Effective CT & MRI Contrast Agents

**FRESENIUS
KABI**

[WATCH VIDEO](#)

AJNR

Digital Myelography of Spinal Dysraphism in Infancy: Preliminary Results

P. D. Barnes, A. F. Reynolds, D. C. Galloway, M. Pollay, J. C. Leonard and J. R. Prince

AJNR Am J Neuroradiol 1984, 5 (2) 208-211

<http://www.ajnr.org/content/5/2/208.citation>

This information is current as
of June 9, 2025.

Digital Myelography of Spinal Dysraphism in Infancy: Preliminary Results

P. D. Barnes,¹ A. F. Reynolds,² D. C. Galloway,¹ M. Pollay,² J. C. Leonard,¹ and J. R. Prince¹

Digital techniques are becoming well established as cost-effective for vascular imaging in neuroradiology [1, 2]. Pediatric application of this technology is also under development [3]. Furthermore, there has been increasing use of more efficient, less invasive methods of evaluating pediatric spine problems through newer-generation computed tomography (CT), including scanned-projection radiography, in an attempt to achieve the high contrast resolution of film-screen myelography [4, 5].

For the past 2 years, we have used metrizamide myelography with simple, thick-section polytomography (myelotomography) to evaluate patients with spinal dysraphism. This technique has provided separation of simultaneously imaged bone and neural landmarks in standard surgical planes, while directing CT for specific transaxial plane imaging. It also allows reduction in metrizamide dosage and total radiation exposure as compared with previously used myelographic procedures employing multiple plain filming plus complex thin-section tomography. Further, myelotomography produces high-contrast-resolution imaging superior to CT with reformatting [6]. For further reductions in risk and cost, digital fluorographic techniques are currently being explored. We describe our preliminary experience with digital myelography in the evaluation of spinal dysraphism in infancy.

Subjects and Methods

During a 6-week period in 1983, four infants (ages 5 days, 10 days, 11 months, and 3 years) with lumbar spinal dysraphism underwent digital myelography using the ADAC DPS 4100 (512 × 512 × 8 matrix)/General Electric Fluoricon 300-MSA 1250 system (4.5 in fluoroscopic mode with 0.3 mm focal spot). After this, metrizamide myelotomography was done using the Philips U3-Polytome (10° circular mode). CT was done in three infants using the Varian V-360-3.

All infants received oral hydration before myelography. The three younger infants were sedated with chloral hydrate 50 mg/kg orally, and the older infant with meperidine 40 mg (0.5 mg/kg) and Vistaril

20 mg (0.23 mg/kg) intramuscularly. Spinal puncture was done with a 25 gauge styleted needle (Cook DPNH 325082) at the L4 or L5 level, and 1.5–2.5 ml of cerebrospinal fluid (CSF) was removed.

For each patient, the digital imaging procedure was carried out as follows. With the patient in the left lateral decubitus position, head-up 10°, and spinal needle in place, a single-frame mask image was obtained of the lateral lumbar region at the level of the dysraphic anomaly. Immediately, 1–2 ml of 57–85 mg I/ml metrizamide was rapidly injected, followed by single-frame subtraction imaging to remove superimposed bone. Subsequently, another 2–4 ml of 170 mg I/ml solution was instilled, and the patient was gently turned side-to-side to achieve adequate contrast-CSF mixing for nonsubtraction imaging in the lateral and frontal projections. Image manipulation techniques included gray-scale window selection and inversion, re-registration of subtracted images, edge enhancement, and magnification.

Without additional contrast injection, frontal and lateral myelotomography was done at the same levels followed by CT (five to 15 10-mm-thick slices with 2 mm overlapping). Exposure parameters for digital myelography were 1.65–4.13 mAs at 55–70 kV per exposure. For myelotomography, the factors were 60–90 mAs at 50–65 kV per exposure (2.5 mm Al filtration). For CT, 90–150 mAs at 120 kV per slice was used. Thermoluminescent dosimetry of the midline lower abdomen was done in the fourth patient for skin-level radiation exposure comparisons and confirmed with MDH-R meter-phantom measurements. All patients were observed for adverse effects over the 48 hr after the procedure.

Results

In the first patient (fig. 1), subtracted digital myelography demonstrated the myelomeningocele sac and emerging nerve roots with excellent clarity, though the spinal cord and conus medullaris were less well delineated due to layering of the higher specific-gravity metrizamide (170 mg I/ml) along the dependent side of the subarachnoid space. This was corrected in subsequent applications through more rapid injection of lower-concentration metrizamide (57–85 mg I/ml). Nonsubtraction images showed somewhat better delineation

This article appears in the March/April 1984 issue of *AJNR* and the June 1984 issue of *AJR*.

Received June 1, 1983; accepted after revision September 12, 1983.

Presented in part at the annual meeting of the Society for Pediatric Radiology, Atlanta, April 1983.

¹ Department of Radiology, Oklahoma Children's Memorial Hospital and Veterans' Administration Medical Center, University of Oklahoma Health Sciences Center, Oklahoma City, OK 73126. Address reprint requests to P. D. Barnes, Radiology, Oklahoma Children's Memorial Hospital, P.O. Box 26307, Oklahoma City, OK 73126.

² Department of Neurosurgery, Oklahoma Children's Memorial Hospital and Veterans' Administration Medical Center, University of Oklahoma Health Sciences Center, Oklahoma City, OK 73126.

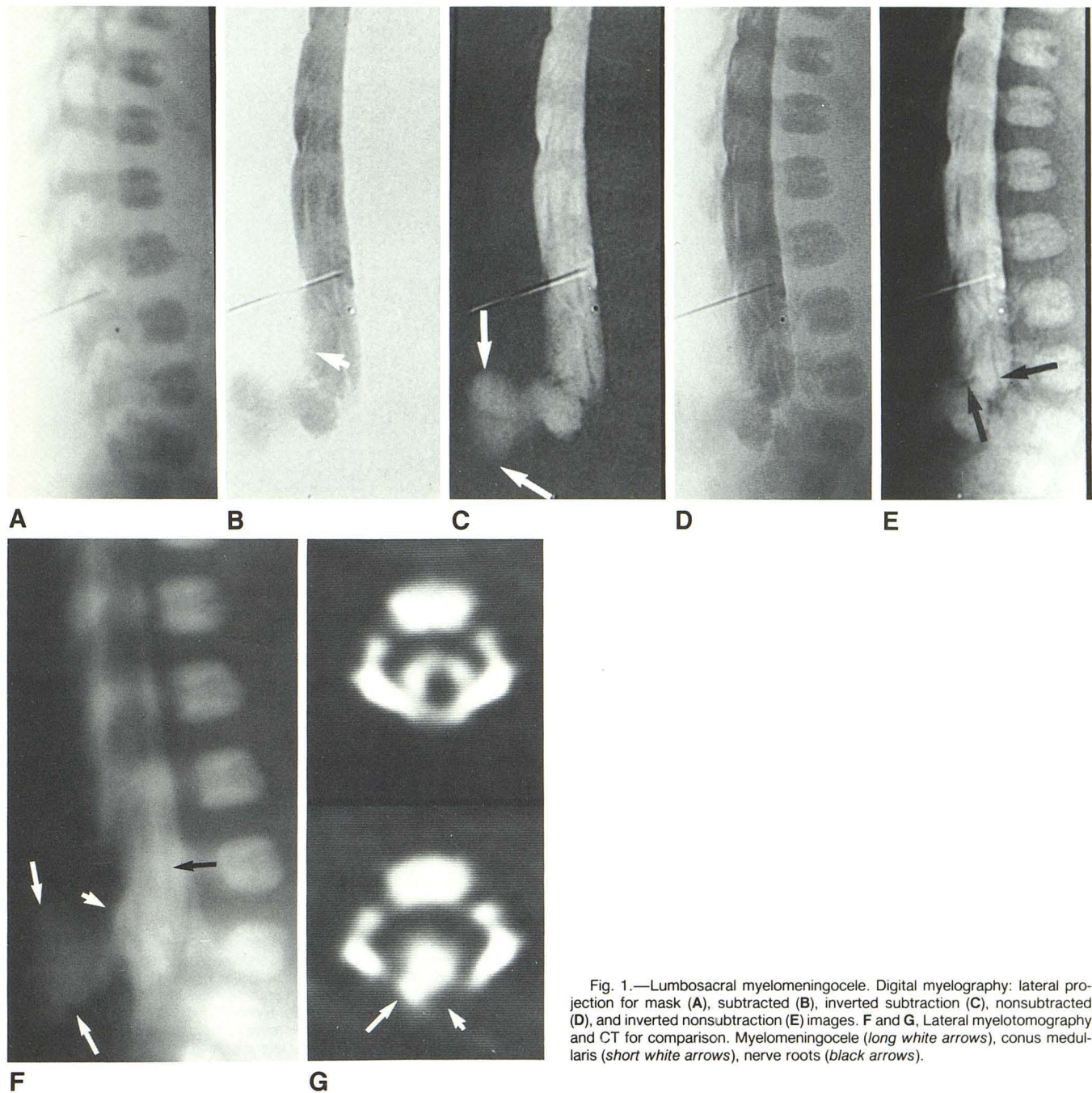


Fig. 1.—Lumbosacral myelomeningocele. Digital myelography: lateral projection for mask (A), subtracted (B), inverted subtraction (C), nonsubtracted (D), and inverted nonsubtraction (E) images. F and G, Lateral myelotomography and CT for comparison. Myelomeningocele (long white arrows), conus medullaris (short white arrows), nerve roots (black arrows).

of the cord and conus at its insertion into the sac. In the second patient (fig. 2), subtraction images were of excellent clarity in demonstrating the low-lying conus medullaris and thickened filum terminale, while nonsubtraction images provided a high-quality survey of the entire spinal neuraxis.

Even though complex-motion misregistration prevented comparable delineation in the other two patients (not shown), the nonsubtracted frames allowed very good clarity of neural structures as displayed through the overlying bone utilizing variable window selection and edge enhancement. This also facilitated specific-level CT imaging in these two infants.

Subtraction digital myelography required rapid injection of only 1–2 ml of hypotonic metrizamide, while nonsubtraction frames required only an additional 1–2 ml and 2–4 ml of isotonic solution for regional and total spinal examination, respectively. In each of the examinations, the time required for image production and review of digital myelograms was less than 10 min. The time required for myelotomography and CT exceeded 30 min each. Hard-copy recording of digital myelography required only single-, six-, or nine-image 10 × 14 inch (25 × 36 cm) film, comparable to that for CT. Myelotomography required six to 10, 8 × 10 inch (20 × 25 cm)

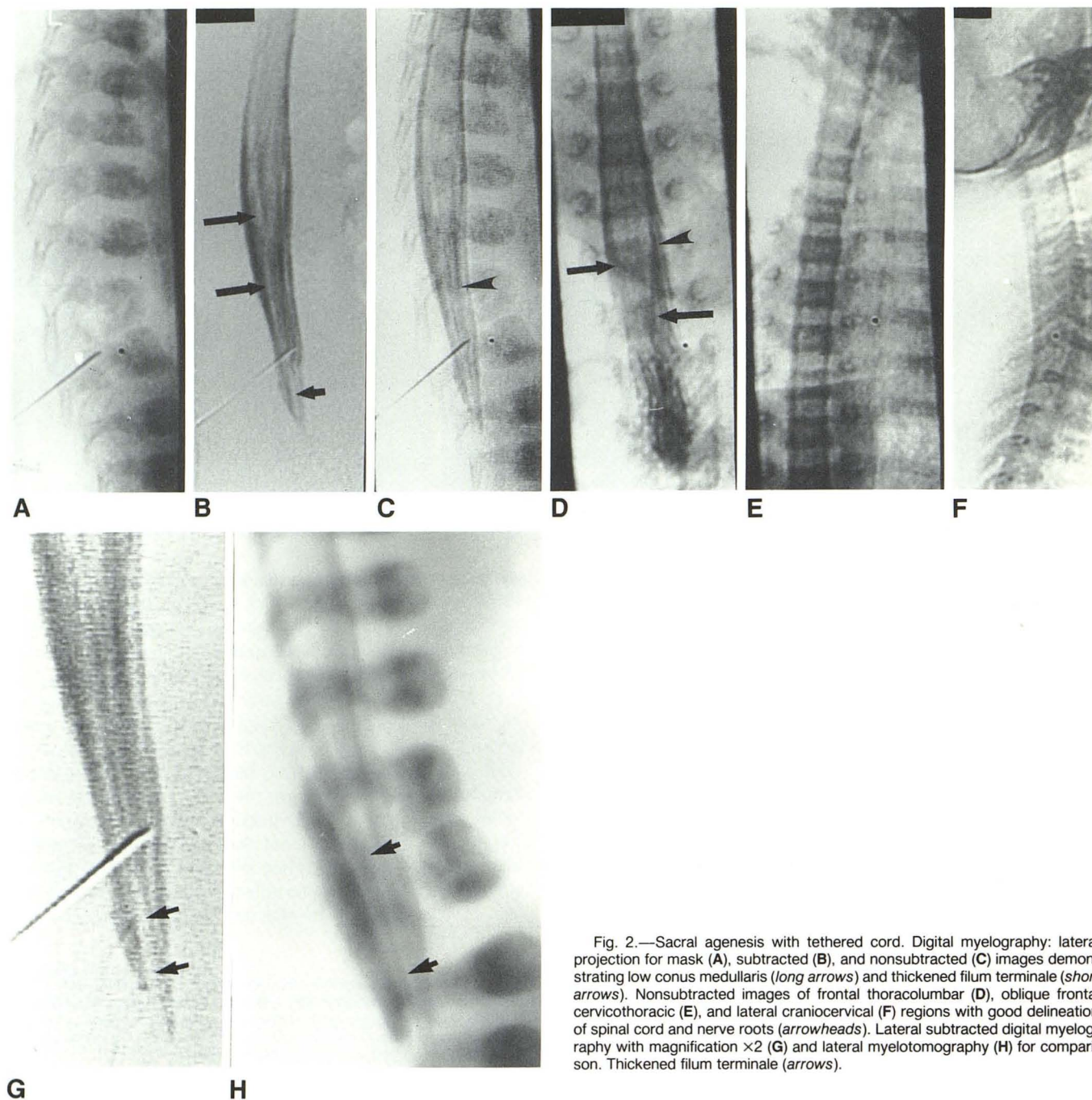


Fig. 2.—Sacral agenesis with tethered cord. Digital myelography: lateral projection for mask (A), subtracted (B), and nonsubtracted (C) images demonstrating low conus medullaris (*long arrows*) and thickened filum terminale (*short arrows*). Nonsubtracted images of frontal thoracolumbar (D), oblique frontal cervicothoracic (E), and lateral craniocervical (F) regions with good delineation of spinal cord and nerve roots (*arrowheads*). Lateral subtracted digital myelography with magnification $\times 2$ (G) and lateral myelotomography (H) for comparison. Thickened filum terminale (*arrows*).

films. The dosimetry data obtained during examination of the fourth child indicates that the integrated radiation exposure dose for digital myelography of 456 mR (1.18 C/kg) for four exposures at 4.13 mAs and 70 kV was comparable to that for plain filming in this patient; was about half that for myelotomography, 992 mR (2.6 C/kg) for four exposures at 90 mAs and 52 kV; and was half that for CT, 980 mR (2.5 C/kg) for seven overlapping sections at 90 mAs and 120 kV. None of the four infants were observed to have any adverse effect from the procedure.

Discussion

Pettersson and Harwood-Nash [7] recently speculated on the cost-effective potential of digital imaging as a future replacement of conventional myelography in providing a survey of the spinal canal and as a guide for the CT examination. Our preliminary experience in four infants with dysraphic myelodysplasia indicates that digital techniques can produce high-contrast-resolution imaging of both bony and neural elements through enhanced contrast sensitivity, as compared

with myelotomography and CT. Digital myelography required smaller volumes of low-concentration metrizamide than did myelotomography, and at an optimal level for immediate CT imaging and analysis. It required less time and less radiation exposure than myelotomography, or for "complete" CT evaluation. In three infants, digital myelography guided the CT for specific-level, low-contrast-resolution imaging and tissue-density characterization, thus promoting efficient use of CT's greatest assets. With continued development of digital technology, it is anticipated that total evaluation of the pediatric spine will be facilitated by sequential "scout" imaging for bony abnormalities, thus replacing plain radiography and at the same time providing "mask" imaging for high-quality subtraction myelography. Furthermore, with the availability of high-resolution sonography [8], it is expected that initial sonographic screening followed by more definitive digital myelography and CT will be the imaging approach for evaluating neonates and young infants with suspected dysraphic myelodysplasia. Ultimately, nuclear magnetic resonance imaging may succeed these methods [9].

ACKNOWLEDGMENTS

We thank J. J. Vanhoutte, B. Eaton, R. Sexton, S. Laws, K. Phillips, J. Bates, N. Brugmann, R. Raftery, B. Weist, S. Burns, R. Lewis, and C. Hendricks for technical assistance; Catherine Remey for manuscript preparation; and Carolyn Martel for illustrations.

REFERENCES

1. Brant-Zawadzki M, Gould R, Norman D, Newton TH, Lane B. Digital subtraction cerebral angiography by intra-arterial injection: comparison with conventional angiography. *AJNR* **1982**;3:593-599, *AJR* **1983**;140:347-353
2. Wood GW, Lukin RR, Tomsick TA, Chambers AA. Digital subtraction angiography with intravenous injection. Assessment of 1,000 carotid bifurcations. *AJNR* **1983**;4:125-129, *AJR* **1983**;140:855-859
3. Wagner ML, Singleton EB, Egan ME. Digital subtraction angiography in children. *AJR* **1983**;140:127-134
4. Harwood-Nash DC. Computed tomography of the pediatric spine: a protocol for the 1980's. *Radiol Clin North Am* **1981**;19:479-494
5. Fitz CR. Midline anomalies of the brain and spine. *Radiol Clin North Am* **1982**;5:95-104
6. Barnes P. Progress in cost-effective radiological evaluation of pediatric and adolescent neurologic spine disease. Presented at the annual meeting of the Society for Pediatric Radiology, Atlanta, April **1983**
7. Pettersson H, Harwood-Nash DC. *CT and myelography of the spine and cord*. New York: Springer-Verlag, **1982**:111-112
8. Kangaroo H, Diamant MJ, King W. High resolution ultrasonography of the neonatal spine. Presented at the annual meeting of the Society for Pediatric Radiology, Atlanta, April **1983**
9. Modic MT, Weinstein MA, Pavlicek KW, et al. Nuclear magnetic resonance imaging of the spine. *Radiology* **1983**;148:757-762